TISSUE ENGINEERING: Part A
Volume 21, Numbers 3 and 4, 2015

DOI: 10.1089/ten.tea.2013.0673

# Systemic Infusion of Mesenchymal Stem Cells Improves Cell-Based Bone Regeneration via Upregulation of Regulatory T Cells

Yi Liu, PhD,[1] Ruili Yang, PhD,[2] and Songtao Shi, DDS, PhD[2]

Mesenchymal-stem-cell-based regenerative medicine is a promising approach for functional tissue reconstruction. A recent study showed that host immune cells regulated bone marrow mesenchymal stem cell (BMMSC)–mediated tissue regeneration. However, it is unknown whether systemic infusion of BMMSCs, which induces immune tolerance, affects cell-based tissue regeneration. In this study, we showed that BMMSCs possessed an immunomodulatory function *in vitro*. Moreover, systemic infusion of BMMSCs reduced IFN-γ and TNF-α levels in the implantation sites via upregulation of regulatory T cells (Tregs), resulting in marked enhancement of cell-based bone regeneration, but with only limited contribution by BMMSC homing. Further, we showed that systemic BMMSC infusion significantly improved cell-based repair of critical-sized calvarial defects in a murine model. These results suggested a new approach to enhance cell-based bone regeneration.

## Introduction

Bone marrow mesenchymal stem cells (BMMSCs) are nonhematopoietic multipotent stem cells and express CD73, CD90, CD146, CD105, Stro-1, stem cell antigen-1 (Sca-1), octamer-binding transcription factor-4 (Oct-4), and pericyte-associated antigen (3G5), but surface molecules CD34, CD45, CD14, and CD11b are absent.[1,2] BMMSCs are also capable of differentiating into both mesenchymal and nonmesenchymal cell types, including osteoblasts, adipocytes, chondrocytes, and neural cells,[3–7] as well as secreting soluble factors to regulate crucial biological functions.[8–10] When implanted *in vivo*, BMMSCs form bone and induce recipient cells to form hematopoietic marrow components.[11,12] Based on these properties, BMMSCs are considered a promising cell source for regenerative medicine in terms of forming bone and hematopoietic marrow structures.

To date, a variety of preclinical and clinical studies have shown that BMMSCs can generate bone to replace damaged and diseased tissues.[13–16] On the other hand, the recipient immunological system also plays a critical role in BMMSC-mediated regeneration. Specifically, interleukin-2 (IL-2)–activated NK cells and CD3/CD28-activated T cells are able to induce BMMSC apoptosis.[17–19] Thus, interaction between recipient immune cells and implanted BMMSCs may affect the fate of implanted BMMSCs and their capacity for tissue regeneration.

In previous studies, we have found that BMMSC-mediated bone regeneration was partially controlled by the recipient local microenvironment in which immune cells and cytokines affected the BMMSCs.[17,19] Proinflammatory T cells inhibited the ability of exogenously added BMMSCs to mediate bone repair. This inhibition was due to interferon γ (IFN-γ)–induced downregulation of the runt-related transcription factor 2 (Runx-2) pathway and enhancement of tumor necrosis factor α (TNF-α) signaling to induce BMMSC apoptosis. Systemic infusion of $CD4^+CD25^+$ $Foxp3^+$ Tregs was able to inhibit activated T cells to induce immune tolerance, which, in turn, promote cell-based bone formation *in vivo*.[17]

It has been recently reported that BMMSCs possess immunomodulatory properties capable of interacting with several subsets of immune cells, such as T cells, B cells, dendritic cells, and natural killer cells.[20–22] These immunosuppressive functions make BMMSCs of great interest for clinical applications in treating a variety of human diseases, including acute graft-versus-host disease and systemic lupus erythematous, as well as promoting hematopoietic stem cell engraftment.[23–25] However, whether the immunoregulatory capacity of BMMSCs also could be used to improve the bone regeneration *in vivo* was unknown. The purpose of this study was to investigate whether systemic infusion of BMMSCs could promote cell-based bone formation in C57BL/6J wild-type mice via immunoregulatory capacity of BMMSCs.

[1]Laboratory of Tissue Regeneration and Immunology and Department of Periodontics, Beijing Key Laboratory for Tooth Regeneration and Function Reconstruction, Capital Medical University School of Stomatology, Beijing, China.
[2]Center for Craniofacial Molecular Biology, University of Southern California, Los Angeles, California.

## Materials and Methods

### Animals

Female C3H/HeJ, C57BL/6J, and C57BL/6-Tg (ACTB-EGFP)1Osb/J mice were purchased from the Jackson Lab. Female immunocompromised mice (Beige *nude/nude* XI-DIII) were purchased from Harlan. All animal experiments were performed under the institutionally approved protocols for the use of animal research (University of Southern California protocol Nos. 10874 and 10941). Mice strain, sex, age, and numbers in all of the experiments are shown in Table 1.

### Isolation of mouse BMMSCs

Bone marrow cells were flashed out from bone cavity of femurs and tibias with 2% heat-inactivated fetal bovine serum (FBS; Equitech-Bio) in phosphate-buffered saline (PBS). Single-cell suspension of all nuclear cells was obtained by passing all bone marrow cells through a 70-μm cell strainer (BD Bioscience); then, $10–15\times10^6$ cells were seeded onto 100-mm culture dishes (Corning) and initially incubated for 48 h under 37°C at 5% $CO_2$ condition. To eliminate the nonadherent cells, the cultures were washed with PBS twice. The attached cells were cultured for 16 days. Colony-forming attached cells were passed once for further experimental use. The BMMSCs were cultured with alpha minimum essential medium (α-MEM; Invitrogen Corporation) supplemented with 20% FBS, 2 mM L-glutamine (Invitrogen Corporation), 55 μM 2-mercaptoethanol (Invitrogen Corporation), 100 U/mL penicillin, and 100 μg/mL streptomycin (Invitrogen Corporation). To confirm mesenchymal stem cell phenotypes, we used flow cytometric analysis to show that these BMMSCs were positive for CD73, CD90, CD105, CD146, CD166, Sca-1, and SSEA-4, but negative for CD11b, CD31, CD34, and CD45.

### T lymphocyte isolation

Spleen Pan T and $CD4^+CD25^-$ T lymphocytes were isolated from total spleen cells of female 8-week-old C57BL/6J mice using a magnetic sorter, mouse Pan T cell isolation kit II, and $CD4^+CD25^+$ regulatory T cell isolation kit (Miltenyi Biotec) following the manufacturer's instructions.

### Coculture of BMMSCs and Spleen Pan T cells

To activate Pan T cells, mouse naive T lymphocytes ($1\times10^6$ per well) were precultured on 24-well multiplates with T cell culture medium in the presence of plate-bound anti-CD3ε antibody (2 μg/mL; Santa Cruz) and soluble anti-CD28 antibody (2 μg/mL; Santa Cruz) for 2–3 days. T cell culture medium included Dulbecco's modified Eagle's medium (DMEM; Lonza, Inc.) with 10% heat-inactivated FBS, 50 μM 2-mercaptoethanol, 10 mM HEPES (Sigma-Aldrich), 1 mM sodium pyruvate (Sigma-Aldrich), 1% nonessential amino acid (Lonza, Inc.), 2 mM L-glutamine, 100 U/mL penicillin, and 100 mg/mL streptomycin. Then, activated Pan T cells ($1\times10^6$/well) were cocultured with $0.2\times10^6$ BMMSCs on 24-well multiplates for another 3 days with T cell culture medium. After 3 days, cells in suspension were collected. The apoptotic T cells were detected by staining with CD3 antibody (eBioscience), followed by Annexin-V Apoptosis Detection Kit I (BD Bioscience) according to manufacturer's protocol, and analyzed by $FACS^{Calibur}$ (BD Bioscience).

### In vitro *Th1 and Th2 induction by BMMSCs*

Activated Pan T cells ($1\times10^6$/well) were cocultured with $0.2\times10^6$ BMMSCs on 24-well multiplates for 3 days with T cell culture medium. After 3 days, cells in suspension were collected and detected Th1 and Th2. The cells ($1\times10^6$) were treated with anti-CD4-PerCP (eBioscience) for 45 min on ice under dark condition and then stained with anti-IFN-γ-PE (eBioscience) or anti-IL-4-PE antibody (1 μg/mL) (eBioscience) after cell fixation and permeabilization using Foxp3 staining buffer kit according to the manufacturer's protocol (eBioscience). All samples were analyzed with $FACS^{Calibur}$ (BD Bioscience). The concentrations of IFN-γ, TNF-α, and IL-4 in supernatant were analyzed by ELISA Ready-SET-GO kits (eBioscience).

### In vitro *Tregs and Th17 induction by BMMSCs*

$CD4^+CD25^-$T-lymphocytes ($1\times10^6$/well) were activated on 24-well multiplates with T cell culture medium in the presence of plate-bound anti-CD3ε antibody (5 μg/mL) and soluble anti-CD28 antibody (2 μg/mL) for 3 days. Then, these activated T-lymphocytes ($1\times10^6$/well) were cocultured with $0.2\times10^6$ BMMSCs on 24-well multiplates with T cell-induced medium for 3 days. For Treg induction, recombinant mouse TGF-β1 (2 μg/mL; R&D Systems) and IL-2 (2 μg/mL; R&D Systems) were added. After 3 days, cells in suspension were collected and stained to detect Tregs. The cells ($1\times10^6$) were treated with anti-CD4-PerCP and anti-CD25-APC antibodies (each 1 μg/mL; eBioscience) for 45 min on ice under dark condition. Cells were then stained with anti-Foxp3-PE antibody (1 μg/mL), using a Foxp3 staining buffer kit (eBioscience) for cell fixation and permeabilization, according to the manufacturer's protocol. The cells were analyzed by using $FACS^{Calibur}$ (BD Bioscience). The supernatant was collected to analyze IL-10 levels by enzyme-linked immunosorbent assay (ELISA), following the manufacturer's instructions.

For Th17 induction, recombinant mouse TGF-β1 (2 μg/mL) and IL-6 (50 μg/mL; R&D Systems) were added. After 3 days, cells in suspension were collected and stained to detect Th17. The cells ($1\times10^6$) were treated with anti-CD4-PerCP antibody (each 1 μg/mL) for 45 min on ice under dark condition. Cells were then stained with anti-IL-17-PE antibody (1 μg/mL), using a Foxp3 staining buffer kit (eBioscience) for cell fixation and permeabilization, according to the manufacturer's protocol. The cells were analyzed by using $FACS^{Calibur}$ (BD Bioscience). The supernatant was collected to analyze IL-17 levels by ELISA, following the manufacturer's instructions.

### Allogenic mouse BMMSC implantation

Hydroxyapatite/tricalcium phosphate (HA/TCP) ceramic powders (40 mg; Zimmer, Inc.) were maintained with α-MEM in a 1.5-mL tube for 30 min at 37°C. Approximately $4.0\times10^6$ of C3H/HeJ-derived BMMSC suspension (1 mL) were added on the powder, incubated for 1.5 h, and gently agitated every 30 min to allow cell attachment. Then, the

Table 1. Animal Use in the Experiments

| *Experiment* | *Cells* | *Animal strain and total numbers* | *Groups* |
|---|---|---|---|
| Immunomodulation properties of BMMSCs | BMMSCs for coculture | C57BL/6J, female, 8-week-old, 10 mice | Three wells for each group. The experiments were repeated five times |
| T cell apoptosis; Th1, Th2, Th17, and Treg cell induction | T lymphocytes | C57BL/6J, female, 8-week-old, 10 mice | Group 1: naive T cells (negative control)<br>Group 2: active T cells (positive control)<br>Group 3: Coculture BMMSCs with active T cell |
| Allogenic mouse BMMSC implantation | BMMSCs for implants | C3H/HeJ mice, female, 8-week-old, five mice (totally about $8\times10^7$ BMMSCs) | BMMSCs (C3H/HeJ)/HA/TCP were implanted to C57BL/6J mice or immunocompromised mice, harvested at 8 weeks postimplantation |
| | BMMSCs for systemic infusion | C57BL/6J mice, female, 8-week-old one mouse<br>Receipt mice: immunocompromised mice, female, 8-week-old, two mice<br>C57BL/6J mice, female, 8-week-old, nine mice | Group 1: BMMSCs/HA/TCP in immunocompromised mice (five implants in two mice)<br>Group 2: BMMSCs/HA/TCP in C57BL/6J mice (five implants in three mice)<br>Group 3: BMMSCs/HA/TCP in C57BL/6J mice with BMMSCs iv. (five implants in three mice)<br>Group 4: BMMSCs/HA/TCP in C57BL/6J mice with BMMSCs iv. and anti-CD25 antibody (five implants in three mice) |
| Cytokine levels | BMMSCs for implants | C3H/HeJ mice, female, 8-week-old, 15 mice (totally about $2.4\times10^8$ BMMSCs) | BMMSCs (C3H/HeJ)/HA/TCP were implanted to C57BL/6J mice; harvested at 2, 4, 7, and 14 days postimplantation; five implants at each time point, one implant per mouse |
| | BMMSCs for systemic infusion | C57BL/6J mice, female, 8-week-old, five mice<br>Receipt mice: C57BL/6J mice, female, 8-week-old, 60 mice | Group 1: HA/TCP in C57BL/6J mice (20 implants in 20 mice)<br>Group 2: BMMSCs/HA/TCP in C57BL/6J mice (20 implants in 20 mice)<br>Group 3: BMMSCs/HA/TCP in C57BL/6J mice with BMMSCs iv. (20 implants in 20 mice) |
| Surviving cells in BMMSC implants | BMMSCs for implants (labeled in red color with PKH26) | C3H/HeJ mice, female, 8-week-old, 10 mice (totally about $1.6\times10^8$ BMMSCs) | BMMSCs (C3H/HeJ mice)/gelfoam were implanted to C57BL/6J mice; harvested at 3, 7, 14, and 28 days postimplantation; five implants at each time point, one implant per mouse |
| | BMMSCs for systemic infusion | C57BL/6J mice, female, 8-week-old, three mice<br>Receipt mice: C57BL/6J mice, female, 8-week-old, 40 mice | Group 1: BMMSCs/gelfoam in C57BL/6J mice (20 implants in 20 mice)<br>Group 2: BMMSCs/gelfoam in C57BL/6J mice with BMMSCs iv. (20 implants in 20 mice) |

(*continued*)

Table 1. (Continued)

| *Experiment* | *Cells* | *Animal strain and total numbers* | *Groups* |
|---|---|---|---|
| Anti-ALP and TRAP double staining | BMMSCs for implants | C3H/HeJ mice, female, 8-week-old, three mice (totally about $4\times10^7$ BMMSCs) | BMMSCs (C3H/HeJ mice)/HA/TCP were implanted to C57BL/6J mice, harvested at 3 weeks postimplantation, one implant per mouse |
| | BMMSCs for systemic infusion | C57BL/6J mice, female, 8-week-old, one mice<br>Receipt mice: C57BL/6J mice, female, 8-week-old, 10 mice | Group 1: BMMSCs/HA/TCP in C57BL/6J mice (five implants in five mice)<br>Group 2: BMMSCs/HA/TCP in C57BL/6J mice with BMMSCs iv. (five implants in five mice) |
| Homing of systemic infused BMMSCs to implants | BMMSCs for implants | C3H/HeJ mice, female, 8-week-old, five mice (totally about $8\times10^7$ BMMSCs) | Group 1: BMMSCs (C3H/HeJ mice)/gelfoam were implanted to C57BL/6J mice after BMMSCs[C57BL/6-Tg (ACTB-EGFP)1Osb/J] iv., and harvested at the first day postimplantation (five implants in five mice) |
| | BMMSCs for systemic infusion | C57BL/6-Tg (ACTB-EGFP)1Osb/J, female, 8-week-old, five mice<br>Receipt mice: C57BL/6J mice, female, 8-week-old, 20 mice | Group 2: same as group 1, and harvested at the third day postimplantation (five implants in five mice)<br>Group 3: same as group 1, and harvested at the fifth day postimplantation (five implants in five mice)<br>Group 4: same as group 1, and harvested at the seventh day postimplantation (five implants in five mice) |
| Calvarial defect reparation | BMMSCs for reparation | C57BL/6J mice, female, 8-week-old, four mice (totally about $6\times10^7$ BMMSCs) | Group 1: HA/TCP were implanted to calvarial defects of C57BL/6J mice (five mice) |
| | BMMSCs for systemic infusion | C57BL/6J mice, female, 8-week-old, two mice<br>Receipt mice: C57BL/6J mice, female, 8-week-old, 15 mice | Group 2: BMMSCs (C57BL/6J mice)/HA/TCP were implanted to calvarial defects of C57BL/6J mice (five mice)<br>Group 3: BMMSCs (C57BL/6J mice)/HA/TCP were implanted to calvarial defects of C57BL/6J mice after BMMSCs iv. (five mice) |

BMMSCs iv., mean systemic infusion of BMMSCs via tail vein.
BMMSC, bone marrow mesenchymal stem cell; HA/TCP, hydroxyapatite/tricalcium phosphate.

tubes with BMMSCs/HA/TCP were centrifuged at 300 *g* for 10 min. After removing the supernatant, the BMMSCs with HA/TCP were subcutaneously transplanted into the dorsal surface of 8-week-old C57BL/6J mice for 8 weeks. Implants in immunocompromised mice were used as control (see Table 1 for the groups and number of animals used in each group, under ''allogenic mouse BMMSC implantation''). At 8 weeks post-transplantation, the implants were harvested, fixed in 4% PFA, and then decalcified with 5% ethylenediaminetetraacetic acid (EDTA; pH 7.4), followed by paraffin embedding. The paraffin sections were stained with hematoxylin and eosin (H&E). In the systemic BMMSC-infused group, approximately $1.0\times10^6$ BMMSCs were mixed in 200 μL PBS and injected into the mice via tail vein 2 days before implantation. In the Treg-blocked group, 1 mg of anti-mouse CD25 antibody was injected via tail vein every 2 days at the first month to block Treg level after systemic BMMSC infusion.

Bone formation area was quantified by using stained histological sections. Images were analyzed with Photoshop and ImageJ software. The ratio of all bone formation area on total biomaterial area was measured on five sections at different levels of the biomaterial (near the surface and in the center of biomaterial).

### *Cytokine levels in BMMSC implants*

The cytokine levels in the implants were measured by ELISA kit. Briefly, the implants were harvested at 2, 4, 7, and 14 days postimplantation and were put to the tissue grinder immediately. Two hundred microliters of M-PER mammalian protein extraction reagent (Thermo) was added to the grinder. The implant tissue was grinded with protein extraction reagent and kept on ice for 1 h. Then, the grinded tissue was centrifuged at 4000 *g* for 10 min. After carefully collecting and measuring protein concentration in the supernatant, 100 μg of total proteins in 100 μL assay buffer was added to the 96-well plate and the cytokine levels of IFN-γ, TNF-α, IL-4, IL-6, and IL-10 were measured by using ELISA Ready–SET–GO kit (eBioscience). At each time point, five implants were harvested. The cytokines in each sample were analyzed in three parallel wells.

### *Surviving cells in BMMSC implants*

Approximately $1.0\times10^6$ of C3H/HeJ-derived BMMSCs were labeled in red color with PKH26 Red Fluorescent Cell Linker Mini Kit (Sigma-Aldrich), and seeded to Gelfoam sized $4\times4\,mm^2$ as a carrier (see Table 1 for the groups and number of animals used in each group, under ''surviving cells in BMMSC implants''). After cultured for 3 days *in vitro*, labeled BMMSCs with Gelfoam were subcutaneously transplanted into the dorsal surface of 8-week-old C57BL/6J mice with or without systemic BMMSC infusion. At each time point of the two groups, five implants were used. At 3, 7, 14, and 28 days postimplantation, the implants were harvested, fixed in 4% PFA, and embedded in optimal cutting temperature compound (OCT). Five frozen sections at different levels (from the surface to the center of the implant) were chosen from each implant, and the ratio of all surviving red cell number on whole section was calculated. The average ratio of the five sections for each implant was analyzed and then the results from all the implants in each group were averaged.

### *Homing of systemic infused BMMSCs to implant*

$GFP^+$ BMMSCs were derived from C57BL/6-Tg (ACTB-EGFP)1Osb/J mice. Approximately $1.0\times10^6$ $GFP^+$ BMMSCs were mixed in 200 μL PBS and injected into the mice via tail vein 2 days before implantation (Gelfoam as a carrier, see Table 1 for the groups and number of animals used in each group, under ''homing of systemic infused BMMSCs to implants''). At 1, 3, 5, and 7 days post-implantation, the implants were harvested, fixed in 4% PFA, and embedded in OCT compound. The ratio of all homing $GFP^+$ cell numbers on whole biomaterial area was calculated on five frozen sections at different levels of the biomaterial (near the surface and in the center of biomaterial).

### *Anti-ALP and TRAP double staining*

The transplants were harvested (see Table 1 for the groups and number of animals used in each group, under ''anti-ALP and TRAP double staining''), fixed in 4% PFA, and then decalcified with 5% EDTA (pH 7.4), followed by paraffin or OCT compound embedding. The paraffin sections were blocked with normal serum and incubated with the specific or isotype-matched primary rabbit anti-mouse ALP antibody (Santa Cruz; 1:200) overnight at 4°C. Then, the samples were stained by using Zymed SuperPicture™ Kit (Invitrogen Corporation) according to manufacturer's instruction. After anti-ALP immunohistochemical staining, the sections were rehydrated and incubated with TRAP staining solution containing 0.1 M acetate buffer, 0.5 M sodium tartrate, 10 mg/mL naphthol AS-MX phosphate, 100 μL Triton X-100, and 0.3 mg/mL Fast Red Violet LB salt for 3 h at 37°C. Sections were then counterstained with hematoxylin before mounting and analyzed by NIH ImageJ. Five paraffin sections at different levels (from the surface to the center of the implant) were chosen from each implant, and the ratio of TRAP-positive cell number or all ALP-positive cell numbers on whole section was calculated. The average ratio of the five sections for each implant was analyzed, and then the results from all the implants in each group were averaged.

### *Calvarial bone defect model in C57BL/6J mice*

After exposure of calvarial bone in C57BL/6J mice, an oversized bone defect about $7\times8\,mm^2$ was established. The bone defect was larger than the usual critical size (diameter about 4 mm).

### *Implantation of BMMSCs to repair calvarial defects in C57BL/6J mice*

When HA/TCP was used as a carrier, approximately $4.0\times10^6$ of C57BL/6J-derived BMMSCs were mixed with HA/TCP ceramic powders (40 mg; Zimmer, Inc.), placed to the calvarial bone defects, and covered completely by skin. For systemic BMMSC-infused group, approximately $1.0\times10^6$ BMMSCs were suspended in 200 μL PBS and injected into the mice via tail vein 2 days before implantation. At 12 weeks posttransplantation, the implants were harvested, fixed in 4% PFA, and then decalcified

with 5% EDTA (pH 7.4), followed by paraffin embedding. The paraffin sections were stained with H&E and analyzed by NIH ImageJ. Five serial sections were selected from the center of the implants. The ratio of all newly formed bone on whole biomaterial area of each section was calculated. Width of left bone defect was shown as a percentage of width of nonrepair calvarial bone defect to original calvarial bone defect. Five implants were analyzed in each group.

### In vivo *$CD4^+$ $CD25^+$ $Foxp3^+$ level after BMMSC infusion*

P1 BMMSCs ($1\times10^6$/mouse) were injected into C57BL/6J mice (10 weeks old, $n=5$, total 30 mice) intravenously (shortly with BMMSC iv.). PBS was injected into age-matched mice as control ($n=5$, total 30 mice). After 0, 2, 4, 7, 14, 21, and 28 days from injection, spleen cells from each group were collected and stained with anti-CD4-PerCP, anti-CD25-APC, and anti-Foxp3-PE antibodies, using Foxp3 staining buffer set (eBioscience) according to the manufacturer's instruction. Samples were analyzed by $FACS^{calibur}$ (BD).

### *Microcomputed tomography analyses*

Calvarial bones were harvested and analyzed by using Inveon microCT system (Siemens AG). Two-dimensional images were analyzed by NIH ImageJ.[12]

### *Statistics*

Student's *t*-test was used to do the statistic analysis when two sets of data followed a normal distribution, which was verified by normality plots. When the data distribution was skewed, Wilcoxon rank-sum test was applied. After verifying the homogeneity of variance and normal distribution of data, the comparisons of multiple variables were carried out using one-way analysis of variance (ANOVA). If the ANOVA was significant, then the Student-Newman-Keuls (SNK) *post hoc* test was performed. Variance equality of data was tested by Levence's test. Rank sum test would be used in case of non-normality of the data or significant differences in variances. $p$-Value $< 0.05$ was considered significant.

## Results

### *BMMSCs inhibited the production of IFN-$\gamma$ and TNF-$\alpha$ from activated T cells* in vitro

To investigate the immunoregulatory capacity of BMMSCs *in vitro*, activated T cells were cocultured with BMMSCs for 48 h. We found that BMMSCs could significantly induce T cell apoptosis (Fig. 1A, $p<0.01$) and inhibit their differentiation into Th1, Th2, and Th17 cells (Fig. 1B–D, $p<0.01$). In contrast, BMMSCs promoted the formation of $CD4^+CD25^+Foxp3^+$ Tregs (Fig. 1E, $p<0.01$). Moreover, ELISAs showed that BMMSCs significantly reduced the levels of T cell-produced IFN-γ, TNF-α, and IL-17 in the supernanant of coculture system when compared with induced T cells (Fig. 1F–H, $p<0.001$), along with an elevated level of IL-10 (Fig. 1I, $p<0.01$). These data confirm that BMMSCs possess *in vitro* immunomodulatory function.

### *Systemic infusion of BMMSCs promoted cell-based osteogenesis in C57BL/6J mice*

We used an established *in vivo* BMMSC implantation system to test whether host immune system affected bone formation in wild-type mice, in which $4\times10^6$ BMMSCs

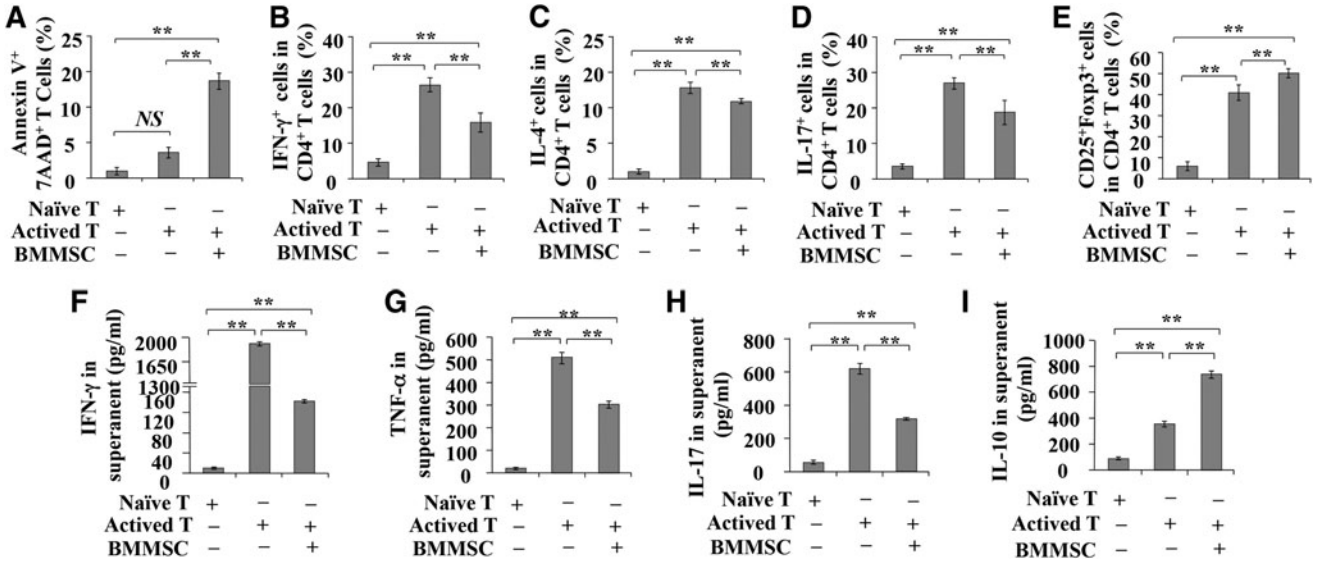


**FIG. 1.** Coculture activated T cells with bone marrow mesenchymal stem cells (BMMSCs). **(A)** The effect of BMMSCs on T cell apoptosis. **(B–E)** The effect of BMMSCs on T cell differentiation. The differentiation of Th1 **(B)**, Th2 **(C)**, and Th17 cells **(D)** was measured by intracellular detection of IFN-γ-, IL-4-, and IL-17-positive cells, respectively, from purified $CD4^+$ T cells in the presence or absence of BMMSCs. The differentiation of Tregs **(E)** was measured by intracellular detection of Foxp3-positive cells, from purified $CD4^+CD25^+$ T cells. **(F–I)** Cytokines levels in the coculture supernatants, including IFN-γ **(F)**, TNF-α **(G)**, IL-17 **(H)**, and IL-10 **(I)**, were determined by ELISA. All the values represent mean ± SEM of five independent experiments. NS, no significant difference, $^{**}p<0.01$.

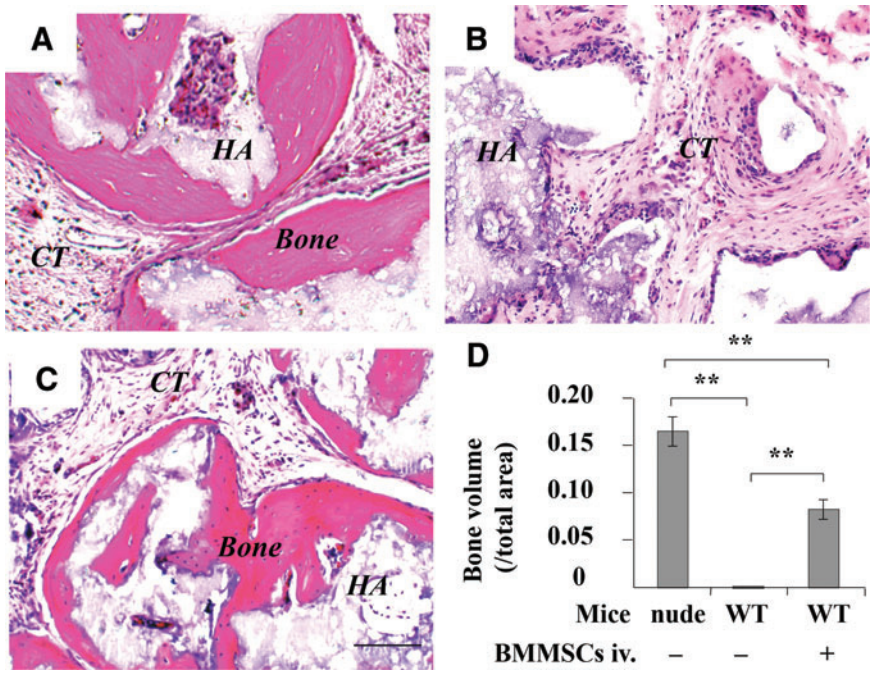


**FIG. 2.** Effect of systemic BMMSC infusion on BMMSC-mediated subcutaneous bone formation in C57BL/6J mice. **(A)** Histological structure of subcutaneous implantation in immunocompromised mice at 8 weeks post-BMMSC/HA/TCP implantation. **(B)** Histological structure of subcutaneous implantation in C57BL/6J mice. **(C)** Histological structure of subcutaneous implantation in C57BL/6J mice after $1 \times 10^6$ BMMSCs systemic infusion. **(D)** ImageJ semiquantitative analysis indicated the amount of bone formation in BMMSC implants. New bone (*Bone*), connective tissue (*CT*), HA/TCP (*HA*), $^{**}p < 0.01$, $n = 5$. Scale bar = 100 μm. HA/TCP, hydroxyapatite/tricalcium phosphate. Color images available online at www.liebertpub.com/tea

with carrier HA/TCP particles were subcutaneously implanted into wild-type C57BL/6J mice for 8 weeks, immunocompromised mice were used as control. Eight weeks later, bone/bone marrow structure could be regenerated in implantation of immunocompromised mice (Fig. 2A), but failed to form bone when C57BL/6J mice were used as recipients (Fig. 2B). To examine whether systemic infusion of BMMSCs affected local BMMSC-mediated bone formation, we infused $1 \times 10^6$ littermate-derived BMMSCs into wild-type C57BL/6J mice via tail vein at 2 days prior to subcutaneous BMMSC implantation. Interestingly, bone tissue was regenerated in wild-type C57BL/6J mice at 8 weeks postimplantation (Fig. 2C), similar to that observed in BMMSC implants of immunocompromised mice (Fig. 2D).

To explore the mechanism causing improved BMMSC-based bone formation *in vivo*, we measured the cytokine levels in C57BL/6J mice after systemic infusion of BMMSCs (Fig. 3A–F). We found that systemic infusion of BMMSCs could reduce the levels of IFN-γ and TNF-α (Fig. 3B, C), but not the levels of IL-4 (Fig. 3D) in BMMSC implants. In addition, systemic infusion of BMMSCs reduced the number of neutrophils (Fig. 3A) and levels of IL-6 (Fig. 3E) in the BMMSC implants at 1–2 and 4–7 days postimplantation, respectively. However, systemic infusion of BMMSCs elevated the level of IL-10 in the BMMSC implants (Fig. 3F). These data indicate that systemic infusion of BMMSCs may promote BMMSC-mediated subcutaneous bone formation, possibly via inhibition of host immune response and reduction of inflammatory cytokines.

Next, we examined whether upregulated Tregs after systemic infusion of BMMSCs played a critical role to improved cell-based bone regeneration. We found that

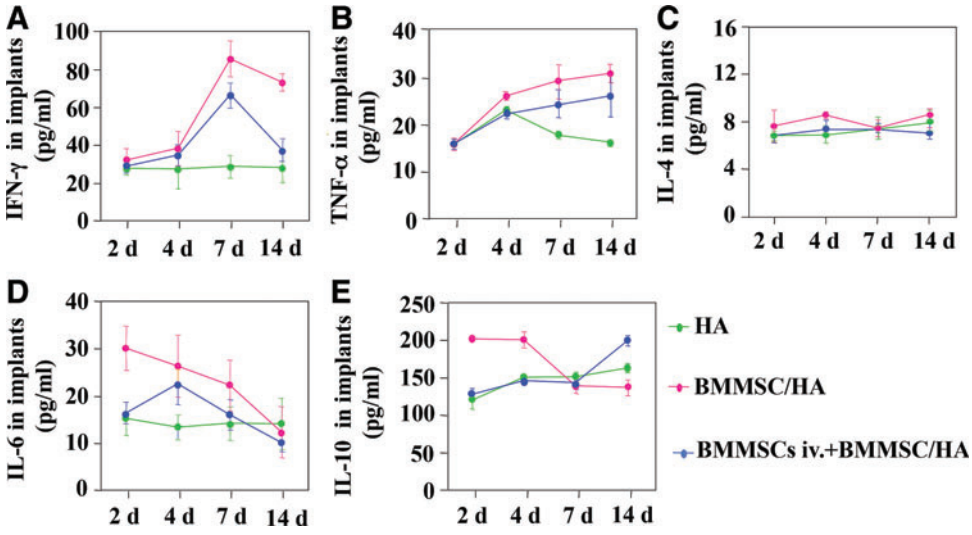


**FIG. 3.** Cytokine production in implantation sites. The levels of IFN-γ **(A)**, TNF-α **(B)**, IL-4 **(C)**, IL-6 **(D)**, and IL-10 **(E)** in the implants at indicated time points. $^{*}p < 0.05$, $^{**}p < 0.01$, $n = 5$. Color images available online at www.liebertpub.com/tea

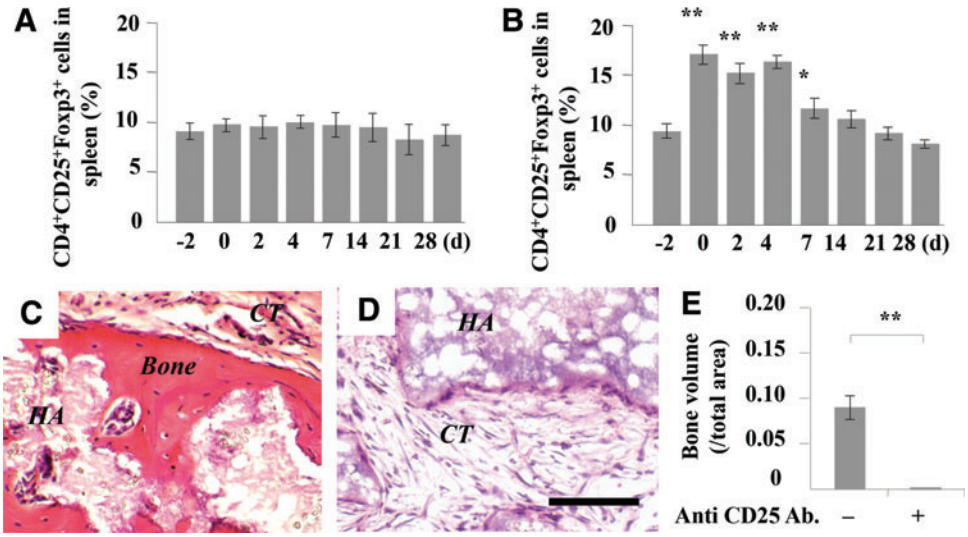


**FIG. 4.** Effect of systemic infusion of BMMSCs on Treg differentiation and BMMSC-mediated subcutaneous bone formation. **(A)** The levels of Tregs in spleen after subcutaneous implantation of BMMSCs. **(B)** The levels of Tregs in spleen of recipient mice after systemic infusion of BMMSCs. **(C)** Histological structure of subcutaneous implantation in C57BL/6J mice after $1\times10^6$ BMMSC systemic infusion. **(D)** Histological structure of subcutaneous implantation when anti-CD25 antibody was used to inhibit the level of Tregs. **(E)** ImageJ semiquantitative analysis indicated the amount of bone formation in BMMSC implants. New bone (*Bone*), connective tissue (*CT*), HA/TCP (*HA*), $*p<0.05$, $**p<0.01$, $n=5$. Scale bar = 100 μm. Color images available online at www.liebertpub.com/tea

subcutaneous implantation of BMMSCs did not affect the level of Tregs in spleen (Fig. 4A). However, systemic infusion of $1\times10^6$ BMMSCs significantly elevated the level of Tregs in recipient spleen, which was reduced to the level observed in control mice at 14 days post-BMMSC infusion (Fig. 4B). Then, LEAF™-purified anti-mouse CD25 antibody was injected to block Tregs after systemic BMMSC infusion (1 mg every 2 days per mouse at the first month, via tail vein); BMMSC-mediated subcutaneous bone formation was abolished in BMMSC implants of C57BL/6J mice (Fig. 4C–E). These data collectively suggest that systemic BMMSC infusion promoted BMMSC-mediated subcutaneous bone formation via elevating the level of Tregs.

### *Systemic infusion of BMMSCs increased the number of surviving cells in BMMSC implants*

When $4\times10^6$ BMMSCs were subcutaneously implanted into C57BL/6J mice, the numbers of surviving BMMSCs in the implants were markedly reduced, and almost no surviving BMMSCs could be detected at 28 days post-implantation (Fig. 5A–E). However, in the systemic

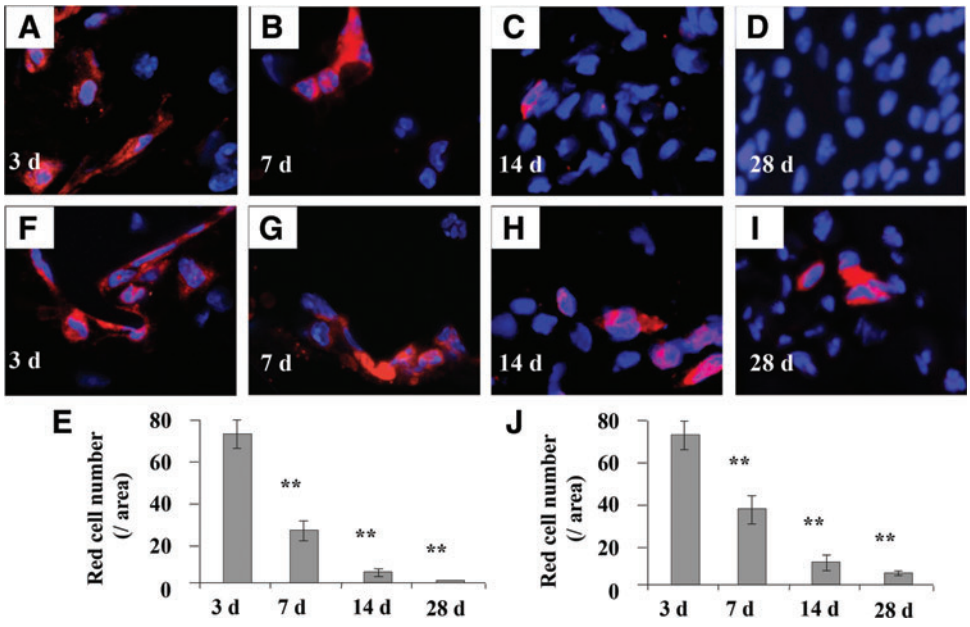


**FIG. 5.** Effect of systemic infusion of BMMSCs on cell survival in BMMSC implants. **(A–D)** The numbers of surviving BMMSCs in implants in C57BL/6J mice. **(E)** Statistical analysis for surviving cells in implants in non-BMMSC infusion group. **(F–I)** The numbers of surviving cells in implants after BMMSC systemic infusion to C57BL/6J recipient. **(J)** Statistical analysis for surviving cells in implants in BMMSC infusion group. $**p<0.01$, $n=5$. Scale bar = 50 μm. Color images available online at www.liebertpub.com/tea

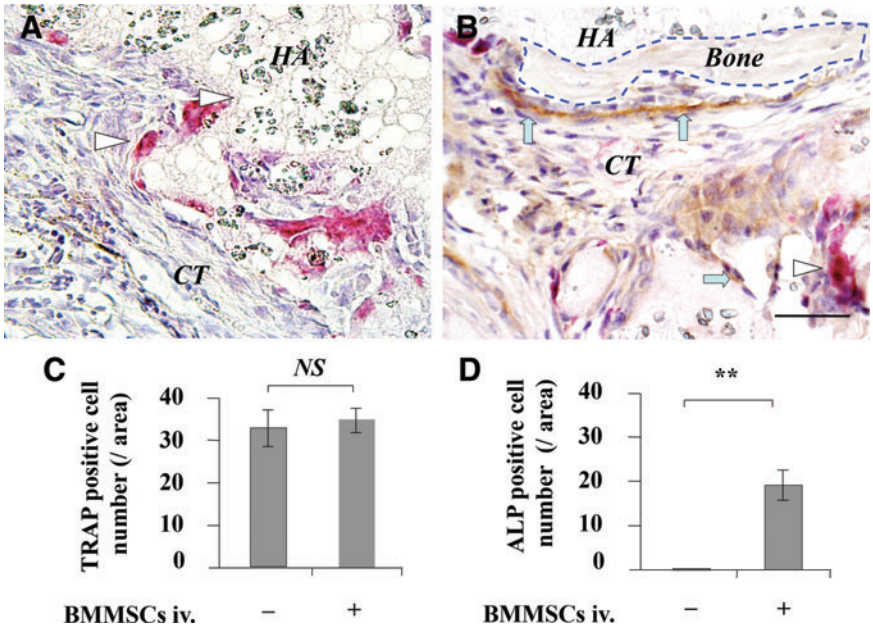


**FIG. 6.** Effect of systemic infusion of BMMSCs on the number of TRAP- and ALP-positive cells in BMMSC implants. The number of osteoclasts and osteoblasts in BMMSC implants was analyzed by TRAP and anti-ALP double staining at 3 weeks post-BMMSC implantation. **(A)** TRAP and anti-ALP staining in group without BMMSC infusion. **(B)** TRAP and anti-ALP staining in BMMSC infusion group. **(C, D)** Statistical analysis for TRAP- and anti-ALP-positive cells in BMMSC implants. *Triangle* showed TRAP-positive cells, *arrow* showed ALP-positive cells, NS, no significant difference, $^{**}p < 0.01$, $n = 5$. Scale bar = 50 μm. Color images available online at www.liebertpub.com/tea

BMMSC infusion group, the number of surviving BMMSCs was much higher than that observed in the untreated control group at 3, 7, 14, and 28 days postimplantation (Fig. 5E–I). At 3 weeks postimplantation, TRAP-positive osteoclasts were observed in both the untreated and BMMSC-infusion groups, but the number of TRAP-positive osteoclasts showed no significant difference between the control and BMMSC-infusion groups (Fig. 6A–C). Additionally, ALP-positive cells were observed in the BMMSC-infusion group, but not in the control group (Fig. 6A, B, D).

### *Systemic infusion of BMMSCs failed to directly contribute to new bone formation via homing in C57BL/6J mice*

To identify whether systemically infused BMMSCs directly contribute to new bone formation in BMMSC implants, we traced the infused BMMSCs in both peripheral blood and implants. After $1 \times 10^6$ BMMSCs were infused via tail vein injection to C57BL/6J mice, very few infused BMMSCs were detected in the implants after the first 5 days (Fig. 7A–C), and they were completely undetectable in BMMSC implants 7 days postimplantation (Fig. 7D, E). These data suggest that infused BMMSCs may not directly home to BMMSC implants to participate new bone formation.

### *Systemic infusion of BMMSCs improved BMMSC-based tissue engineering for repairing calvarial defects in C57BL/6J mice*

Since systemic infusion of BMMSCs inhibited the levels of TNF-α and IFN-γ and promoted bone formation in the implantation site (Fig. 3), we hypothesize that systemic infusion of BMMSCs would improve cell-based tissue engineering for the repair of bone defects. To test this hypothesis,

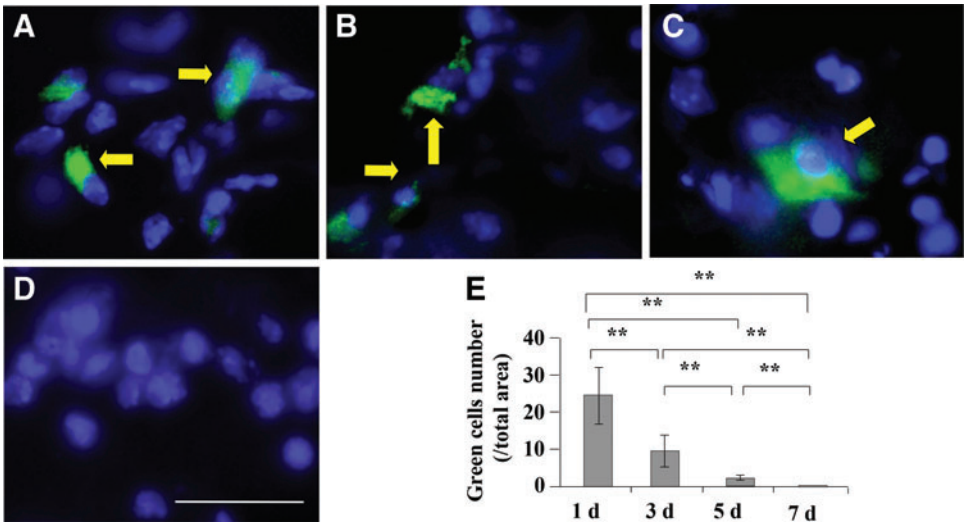


**FIG. 7.** Effect of systemically infused BMMSCs on new bone formation in BMMSC implants in C57BL/6J mice. Systemic infused $GFP^+$ BMMSCs in the implants at one **(A)**, three **(B)**, five **(C)**, and seven **(D)** days postinfusion. **(E)** Statistical analysis for the numbers of systemic infused $GFP^+$ BMMSCs in implants. *Arrow* showed infused BMMSCs. $^{**}p < 0.01$, $n = 5$. Scale bar = 50 μm. Color images available online at www.liebertpub.com/tea

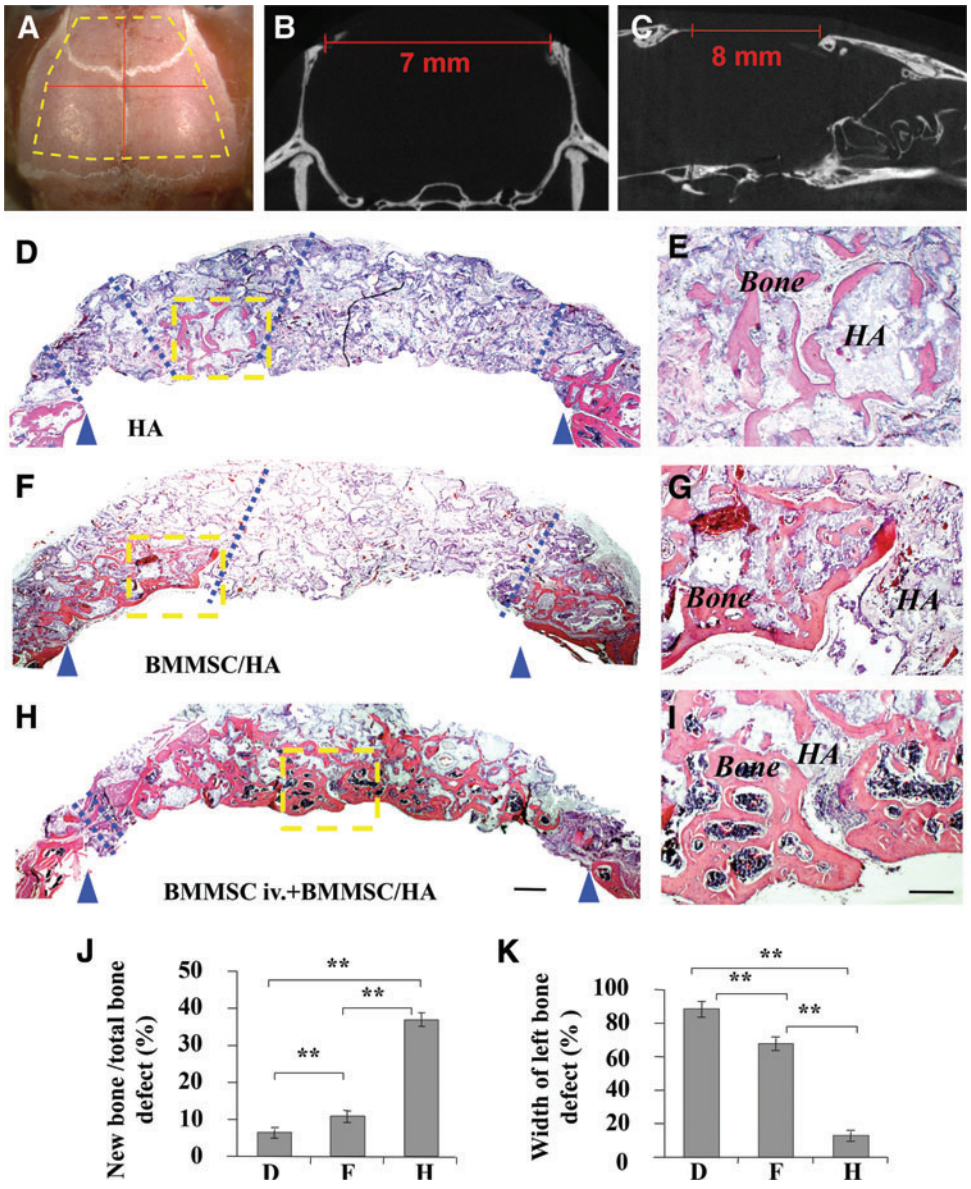


**FIG. 8.** Effect of systemic infusion of BMMSCs on BMMSC-mediated repair of calvarial defects in C57BL/6J mice. **(A–C)** Critical-sized calvarial bone defects of $7\times8\,mm^2$ were generated in C57BL/6J mice. **(D, E)** Histological structure of calvarial bone defect area in control group at 12 weeks postsurgery. **(F, G)** Histological structure of calvarial bone defect area in BMMSC/HA/TCP group. A certain amount of bone formation was noted at 12 weeks postimplantation. **(H, I)** Almost complete repair of the calvarial defects was observed at 12 weeks postimplantation in BMMSC systemic infusion group. **(J)** ImageJ semiquantitative analysis indicated the amount of new bone formation in the three groups. **(K)** Statistical analysis for width of left bone defect. Width of left bone defect (%) = (width between *blue dash lines*/width between *blue triangle arrows*) × 100%. $^{**}p<0.01$, $n=5$. Scale bar = 500 μm in H&E coronal calvarial images of **D**, **F**, and **H**; 200 μm in H&E coronal calvarial images of **E**, **G**, and **I**. H&E, hematoxylin and eosin. Color images available online at www.liebertpub.com/tea

we generated critical-sized calvarial bone defects ($7\times8\,mm^2$) in wild-type C57BL/6J mice and used HA/TCP as a vehicle to carry BMMSCs to repair the bone defect (Fig. 8A–C). The ratio of new bone formation on the total biomaterial area was about 7.4% in the HA/TCP control group at 12 weeks postsurgery, and the width of left bone defect was only about 88.2% (Fig. 8D, E). With implantation of $4\times10^6$ BMMSCs using HA/TCP as a carrier, about 12.1% new bone formation was observed on total biomaterial area at 12 weeks postimplantation, and the width of left bone defect was only about 67.8% (Fig. 8F, G). However, when $1\times10^6$ BMMSCs were systemically infused into the recipient mice via tail vein at 2 days prior to BMMSC ($4\times10^6$)/HA/TCP implantation, almost complete repair of the calvarial defects was observed at 12 weeks postimplantation (Fig. 8H, I). The ratio of new bone formation on total biomaterial area was about 35.7%, and the width of left bone defect was only about 11.3%. ImageJ semiquantitative analysis indicated appropriate amount of new bone formation (Fig. 8J, K). These data imply that upregulation of Tregs by systemic infusion of BMMSCs improves BMMSC-mediated tissue engineering for the repair of calvarial defects.

## Discussion

BMMSCs are considered a unique cell source for potential clinical applications. However, the unstable therapeutic effects and unclear mechanisms of action have limited the advanced application of BMMSCs in tissue engineering. In this study, we found that systemic BMMSC infusion significantly improved cell-based bone regeneration, which suggested a new approach to enhance bone regeneration therapy.

Although BMMSCs showed low immunoantigenicity, the sites of tissue damage always undergo either chronic or acute immune responses. The complex crosstalk between implanted BMMSCs and recipient immune cells in a disease setting plays a key role in determining cell-based bone

regeneration.[17,26,27] Our previous studies suggested that downregulation of the recipient immune system and inflammatory cytokines could significantly improve BMMSC-based bone repair via systemic infusion of Tregs.[17] It is well known that BMMSCs have immunosuppressive and immunomodulatory properties, and are able to interact with almost all subsets of lymphocytes and make them capable of reducing hyperactivated immune responses.[28–32] As such, BMMSCs were used to treat graft-versus-host disease and inflammatory-mediated disorders. In systemic sclerosis mouse models and dextran-sulfate-sodium-induced experimental colitis, BMMSC infusion could induce T cell apoptosis, which leads to a Treg-upregulation-associated immune tolerance that eventually ameliorates the disease phenotype.[24,25,31] In the present study, we showed that BMMSCs possessed *in vitro* immunomodulatory function. BMMSCs were able to induce activated T cell apoptosis and inhibit T cell differentiation into Th1, Th2, and Th17 cells. Moreover, systemic infusion of BMMSCs was able to facilitate BMMSC-based bone regeneration by reducing IFN-$\gamma$ and TNF-$\alpha$ levels in the implantation sites via upregulation of Tregs.

From the results of our study, we found that systemic infused BMMSCs may not directly home to BMMSC implants and act as seed cells to participate the new bone formation. Some studies reported that intravenous injection of BMMSCs was capable of homing to damaged tissue sites, and promoted tissue repair.[33] However, the exact mechanism is unclear. Usually, systemic delivery of *ex-vivo*-expanded BMMSCs through intravenous infusion led to lodging of these BMMSCs mainly in the lungs, with detectable amounts in the liver, heart, and spleen.[34] Thus, although injected BMMSCs showed some capacity to migrate into damaged areas when administered at an early stage, effect of such BMMSCs homing to damaged areas was unclear. Our data suggested that systemically infused BMMSCs were only observed at the early stage in BMMSC implants and that infused BMMSCs became undetectable in BMMSC implants at 7 days postsystemic infusion. Further, when anti-CD25 antibody was used to block the function of Tregs, the new bone formation could not be observed even in systemic BMMSC infusion. These results suggest that systemically infused BMMSCs could improve cell-based bone regeneration mainly through immunomodulation, rather than homing and subsequent osteogenic differentiation inside the implants.[35]

In this study, the functions of systemic infused BMMSCs and site-directly delivered BMMSCs were different. Systemic infused BMMSCs were used to regulate host immune system, but did not directly participate in the bone regeneration process whereas site-directed delivery of BMMSCs with bioscaffold was used as seed cells to repair bone defect. However, the possible roles of BMMSCs in regulating immune and inflammatory responses when delivered locally to regenerate bone tissue are still unclear and deserve more attention.

## Conclusions

Recent advances in stem cell biology and tissue engineering suggest that BMMSC-based tissue regeneration may have promising potential for replacing diseased and damaged tissues. However, it is necessary to clarify the roles of recipient local microenvironment and systemic immune response in cell-based tissue engineering. A better understanding of the relationship between the host immune system and the donor cells will provide a foundation for improving cell-based tissue engineering. Our study indicated that systemic BMMSC infusion significantly improved cell-based repair of critical-sized calvarial defects in a murine model via upregulation of Tregs. These results suggested a new approach to enhance cell-based bone regeneration.

## Acknowledgments

This work was supported by grants from the National Natural Science Foundation of China (81222011 to Y.L.), National Institute of Dental and Craniofacial Research, National Institutes of Health, Department of Health and Human Services (R01DE017449 and R01 DE019932 to S.S.), Science and Technology Activities of Beijing Overseas Students Preferred Foundation (to Y.L.), and the Beijing Key Laboratory Foundation of Science and Technology Special Work (Z121107002812034 to Z.S. and Y.L.).

## Disclosure Statement

There are no known conflicts of interest associated with this publication and there has been no significant financial support for this work that could have influenced its outcome.

## References

1. Bianco, P., and Robey, P.G. Stem cells in tissue engineering. Nature **414,** 118, 2001.
2. Shi, S., and Gronthos, S. Perivascular niche of postnatal mesenchymal stem cells in human bone marrow and dental pulp. JBMR **18,** 696, 2003.
3. Bianco, P., Riminucci, M., Gronthos, S., and Robey, P.G. Bone marrow stromal stem cells: nature, biology, and potential applications. Stem Cells **19,** 180, 2001.
4. Friedenstein, A.J., Chailakhyan, R.K., Latsinik, N.V., Panasyuk, A.F., and Keiliss-Borok, I.V. Stromal cells responsible for transferring the microenvironment of the hemopoietic tissues. Cloning *in vitro* and retransplantation *in vivo*. Transplantation **17,** 331, 1974.
5. Owen, M., and Friedenstein, A.J. Stromal stem cells: marrow-derived osteogenic precursors. Ciba Found Symp **136,** 42, 1988.
6. Pittenger, M.F., Mackay, A.M., Beck, S.C., Jaiswal, R.K., Douglas, R., and Mosca, J.D. Multilineage potential of adult human mesenchymal stem cells. Science **284,** 143, 1999.
7. Prockop, D.J. Marrow stromal cells as stem cells for nonhematopoietic tissues. Science **276,** 71, 1997.
8. Keating, A. Mesenchymal stromal cells: new directions. Cell Stem Cell **10,** 709, 2012.
9. Wu, Y., Chen, L., Scott, P.G., and Tredget, E.E. Mesenchymal stem cells enhance wound healing through differentiation and angiogenesis. Stem Cells **25,** 2648, 2007.
10. Battiwalla, M., and Hematti, P. Mesenchymal stem cells in hematopoietic stem cell transplantation. Cytotherapy **11,** 503, 2009.
11. Krebsbach, P.H., Kuznetsov, S.A., Satomura, K., Emmons, R.V., Rowe, D.W., and Robey, P.G. Bone formation *in vivo*: comparison of osteogenesis by transplanted mouse and human marrow stromal fibroblasts. Transplantation **63,** 1059, 1997.
12. Batouli, S., Miura, M., Brahim, J., Tsutsui, T.W., Fisher, L.W., Gronthos, S., *et al.* Comparison of stem cell-mediated osteogenesis and dentinogenesis. J Den Res **82,** 975, 2003.

13. Caplan, A.I. Adult mesenchymal stem cells for tissue engineering versus regenerative medicine. J Cell Physiol **213,** 341, 2007.
14. García-Gómez, I., Elvira, G., Zapata, A.G., Lamana, M.L., Ramírez, M., Castro, J.G., *et al.* Mesenchymal stem cells: biological properties and clinical applications. Expert Opin Biol Ther **10,** 1453, 2010.
15. Tasso, R., Fais, F., Reverberi, D., Tortelli, F., and Cancedda, R. The recruitment of two consecutive and different waves of host stem/progenitor cells during the development of tissue-engineered bone in a murine model. Biomaterials **31,** 2121, 2010.
16. Bueno, E.M., and Glowacki, J. Cell-free and cell-based approaches for bone regeneration. Nat Rev Rheumatol **5,** 685, 2009.
17. Liu, Y., Wang, L., Kikuiri, T., Akiyama, K., Chen, C., Xu, X., *et al.* Mesenchymal stem cell-based tissue regeneration is governed by recipient T lymphocytes *via* IFN-γ and TNF-α. Nat Med **17,** 1594, 2011.
18. Spaggiari, G.M., Capobianco, A., Becchetti, S., Mingari, M.C., and Moretta, L. Mesenchymal stem cell-natural killer cell interactions: evidence that activated NK cells are capable of killing MSCs, whereas MSCs can inhibit IL-2-induced NK-cell proliferation. Blood **107,** 1484, 2006.
19. Yamaza, T., Miura, Y., Bi, Y., Liu, Y., Akiyama, K., Sonoyama, W., *et al.* Pharmacologic stem cell based intervention as a new approach to osteoporosis treatment in rodents. PLoS One **3,** e2615, 2008.
20. Liu, Y., Wang, S., and Shi, S. The role of recipient T cells in mesenchymal stem cell-based tissue regeneration. Int J Biochem Cell Biol **44,** 2044, 2012.
21. Deans, R.J., and Moseley, A.B. Mesenchymal stem cells: Biology and potential clinical uses. Exp Hematol **28,** 875, 2000.
22. Zhao, S., Wehner, R., Bornhäuser, M., Wassmuth, R., Bachmann, M., and Schmitz, M. Immunomodulatory properties of mesenchymal stromal cells and their therapeutic consequences for immune-mediated disorders. Stem Cells Dev **19,** 607, 2010.
23. Tolar, J., Le Blanc, K., Keating, A., and Blazar, B.R. Concise review: hitting the right spot with mesenchymal stromal cells. Stem Cells **28,** 1446, 2010.
24. English, K., French, A., and Wood, K.J. Mesenchymal stromal cells: facilitators of successful transplantation? Cell Stem Cell **7,** 431, 2010.
25. Sun, L., Akiyama, K., Zhang, H., Yamaza, T., Hou, Y., Zhao, S., *et al.* Mesenchymal stem cell transplantation reverses multi-organ dysfunction in systemic lupus erythematosus mice and humans. Stem Cells **27,** 1421, 2009.
26. Shi, Y., Hu, G., Su, J., Li, W., Chen, Q., Shou, P., *et al.* Mesenchymal stem cells: a. new strategy for immunosuppression and tissue repair. Cell Res **20,** 510, 2010.
27. Raggatt, L.J., and Partridge, N.C. Cellular and molecular mechanisms of bone remodeling. J Biol Chem **285,** 25103, 2010.
28. Krampera, M., Glennie, S., Dyson, J., Scott, D., Laylor, R., Simpson, E., *et al.* Bone marrow mesenchymal stem cells inhibit the response of naive and memory antigen-specific T cells to their cognate peptide. Blood **101,** 3722, 2003.
29. Corcione, A., Benvenuto, F., Ferretti, E., Giunti, D., Cappiello, V., Cazzanti, F., *et al.* Human mesenchymal stem cells modulate B cell functions. Blood **107,** 367, 2006.
30. Jiang, X.X., Zhang, Y., Liu, B., Zhang, S.X., Wu, Y., Yu, X.D., *et al.* Human mesenchymal stem cells inhibit differentiation and function of monocyte-derived dendritic cells. Blood **105,** 4120, 2005.
31. Akiyama, K., Chen, C., Wang, D., Xu, X., Qu, C., Yamaza, T., *et al.* Mesenchymal-stem-cellinduced immunoregulation involves FAS-ligand-/FAS-mediated T cell apoptosis. Cell Stem Cell **10,** 544, 2012.
32. English, K. Mechanisms of mesenchymal stromal cell immunomodulation. Immunol Cell Biol **91,** 19, 2013.
33. Li, Y., Chen, J., Zhang, C.L., Wang, L., Lu, D., Katakowski, M., *et al.* Gliosis and brain remodeling after treatment of stroke in rats with marrow stromal cells. Glia **49,** 407, 2005.
34. Barbash, I.M., Chouraqui, P., Baron, J., Feinberg, M.S., Etzion, S., Tessone, A., *et al.* Systemic delivery of bone marrow-derived mesenchymal stem cells to the infarcted myocardium: feasibility, cell migration, and body distribution. Circulation **108,** 863, 2003.
35. Shen, L.H., Li, Y., Chen, J., Zacharek, A., Gao, Q., Kapke, A., *et al.* Therapeutic benefit of bone marrow stromal cells administered 1 month after stroke. J Cereb Blood Flow Metab **27,** 6, 2006.

Address correspondence to:
*Yi Liu, PhD*
*Laboratory of Tissue Regeneration and Immunology*
*and Department of Periodontics*
*Beijing Key Laboratory for Tooth Regeneration*
*and Function Reconstruction*
*Capital Medical University School of Stomatology*
*Tian Tan Xi Li No. 4*
*Beijing 100050*
*China*

*E-mail:* liuyi@ccmu.edu.cn

*Received: October 31, 2013*
*Accepted: August 25, 2014*
*Online Publication Date: January 16, 2015*